Effective creases and contact angles between membrane domains with high spontaneous curvature

Jean-Baptiste Fournier, Martine Ben Amar

EPJ manuscript No.
(will be inserted by the editor)

Effective creases and contact-angles between membrane domains with high spontaneous curvature

Jean-Baptiste Fournier[1,2] and Martine Ben Amar[3]
[1]Matière et Systèmes Complexes (MSC), UMR 7057 CNRS & Université Paris 7, 2 place Jussieu, F-75251 Paris Cedex 05, France
[2]Laboratoire de Physico-Chimie Théorique, UMR 7083 CNRS & ESPCI, 10 rue Vauquelin, F-75231 Paris Cedex 05, France
[3]Laboratoire de Physique Statistique, École Normale Supérieure, 24 rue Lhomond, F75231 Paris Cedex 05, France

Received: date / Revised version: date

Abstract. We show that the short-scale elastic distortions that are excited in the vicinity of the joint between different lipidic membrane domains (at a scale of $\simeq 10\,\mathrm{nm}$) may produce a "crease" from the point of view of the standard elastic description of membranes, i.e., an effective discontinuity in the membrane slope at the level of Helfrich's theory. This "discontinuity" may be accounted for by introducing a line tension with an effective angular dependence. We show that domains bearing strong spontaneous curvatures, such as biological rafts, should exhibit creases with a finite contact-angle, almost prescribed, corresponding to a steep extremum of the line energy. Finite contact-angles might also occur in symmetric membranes from the recruitment of impurities at the boundary.

PACS. 87.16.Dg Membranes, bilayers, and vesicles – 87.10.+e Biological and medical physics: general theory and mathematical aspects – 68.03.Cd Surface tension and related phenomena

1 Introduction

When phospholipid or like surfactants are dissolved in an aqueous solution, they condensate into fluid bilayer membranes. Lipid bilayers are formed by two contacting monolayers of opposite orientations, in which the hydrophilic heads of the surfactants are directed towards the aqueous solution while the hydrophobic tails, confined within the sheet, are shielded from contact with water [1]. Lipid bilayer membranes are ubiquitous in biological cells [2]. In actual biological systems, membranes are formed of multiple lipid or surfactant components. The latter may laterally separate into coexisting liquid phases, or *domains* [3, 4,5], with distinct compositions and distinct microscopic features, such as the membrane thickness. Microdomains called "rafts" are receiving increasing attention, since they are believed to concentrate proteins that must interact with one another to carry out important cellular functions [6,7].

A number of theoretical works have studied the relationship between the curvature elasticity and line tension of domains and the resulting formation of particular patterns or membrane shapes [8,9,10,11,12,13,14]. In all these works, the *slope* of the membrane is assumed to be *continuous* at the domain boundary. In this paper, we argue that although this assumption is realistic in a large number of situations, it is not correct for domains with strongly asymmetric monolayers, as it is often the case in the biological realm [15].

Here, we need to precise what we mean by a membrane "slope discontinuity" : we mean a discontinuity as far as the standard Helfrich description of membranes is concerned. This "discontinuity" will obviously be resolved at a more microscopic scale, i.e., at the molecular scale or at the scale of more involved elastic theories taking into account short-scale structural degrees of freedom. We do *not* refer here to apparent large-scale discontinuities as, e.g., the "neck" connecting a budding domain in a vesicle [9,10]: these are actually smooth and continuous at a sufficiently short scale within Helfrich's theory. The possibility of actual slope discontinuities in Helfrich's theory, or "creases", was suggested on symmetry grounds for surfactant monolayers in Ref. [16], but not investigated further. Here, we actually study the possibility of such creases in the case of membranes.

At first sight, the condition of a continuous slope across the domain boundary seems mathematically necessary because of the presence of a curvature energy. Indeed, in the standard Helfrich model [17], which describes the membrane as a fluid structureless surface with a curvature elasticity, the energy density is proportional to the square of the membrane curvature. (If the membrane is asymmetric, there also a term linear in the curvature, with a coefficient proportional to the asymmetry of the bilayer.) Within this simple model, which is essentially valid at large length-scales, if one assumes a discontinuous membrane slope at the boundary between two domains, one obtains a localized *infinite* energy (the local energy density

diverges there as the square of a delta-function). However, this reasoning assumes that the Helfrich model may be continuously applied through the boundary between the domains, which is not obvious. In fact, as in every elastic model, there is a cutoff below which Helfrich's model is no longer applicable. The corresponding length-scale is comparable with a few times the membrane thickness, i.e., $\simeq 10$ nm [18]. At the *joint* between membrane domains, there are short-scale elastic degrees of freedom that are excited: matching of the two membrane thicknesses [19, 20], tilt of the lipidic tails [21], etc. These degrees of freedom relax typically on a length scale comparable with the cutoff of the Helfrich model. In this paper, we show that these structural degrees of freedom may result in an apparent *contact-angle* in the large scale Helfrich description (an effective jump in the membrane slope at the joint). We also demonstrate that the energy of these extra degrees of freedom may be "coarse-grained" into an *anisotropic* line energy $\gamma(\theta)$ for the Helfrich model, where θ is the effective slope discontinuity at the joint.

2 Model

Let us consider two contacting membrane domains $\mathcal{D}_i$, $i \in \{1,2\}$. We shall describe them more "microscopically" than in Helfrich's theory. Since we are interested in the local junction between these domains, we assume translational invariance along the y-direction. We take $\mathcal{D}_1 = [-L,0]$ and $\mathcal{D}_2 = [0,L]$, the joint being at $x=0$. Our model free-energy, per unit length, is the following:

$$F = \sum_{i=1,2} \int_{\mathcal{D}_i} dx \left(f_{\rm H}^{(i)} + f_{\rm str}^{(i)} + f_{\rm int}^{(i)} \right) + \gamma_0 \,. \qquad (1)$$

The first contribution $f_{\rm H}^{(i)}$ is similar to the bending energy density of the Helfrich model [17] :

$$f_{\rm H}^{(i)} = \frac{1}{2}\kappa_i \left(\partial^2 h_i\right)^2 - \kappa_i\, c_i\, \partial^2 h_i. \qquad (2)$$

Here $h_i(x)$ represents the height profile of the membrane midplane in domain i. Dealing only with small deformations, we shall neglect everywhere terms of higher-order than h_i^2. With $\partial \equiv d/dx$, the quantity $\partial^2 h_i$ represents the membrane curvature, and κ_i and c_i are the bare bending rigidities and bare spontaneous curvatures, respectively. The latter term, which is linear in h_i, is allowed by symmetry only if the membrane is dissymmetric, i.e., if the lipid or surfactant compositions in the two monolayers are different. For the sake of simplicity, we neglect the surface tensions σ_i, which would give rise to a term of the form $\frac{1}{2}\sigma_i(\partial h_i)^2$: this is reasonable as long as we investigate length scales smaller that $(\kappa_i/\sigma_i)^{1/2}$. Note that the Gaussian rigidities $\bar{\kappa}_i$ [17] can be discarded, since in one dimension the Gaussian curvature vanishes.

The second term, $f_{\rm str}^{(i)}$, arises from the *structural* energy density associated with the inner deformations of the membranes. Although the length-scales under consideration are comparable with a few nanometer, we keep a continuous description. Among the many possible structural variables, two traditional ones are the thickness of the membrane and the tilt of the lipids relative to the membrane's midplane (see, e.g., [21,22]). Note that our aim is not to discuss the most general model, but to show, with the simplest symmetry-allowed terms, the possible existence of the "contact-angle" effect discussed in the introduction. Hence, for the sake of simplicity, we consider only the membrane thickness variable:

$$f_{\rm str}^{(i)} = \frac{1}{2} B_i \left(u_i - a_i\right)^2 + \frac{1}{2} k_i \left(\partial u_i\right)^2 . \qquad (3)$$

Here, $u_i(x)$ describes the thickness of the membrane in domain i. These two terms represent the free-energy cost associated with a variation of u_i with respect to its equilibrium value a_i, at lowest-order in the gradient expansion [22,23,24]. We expect the typical length-scale $(k_i/B_i)^{1/2}$ over which u_i relaxes, i.e., the width of the joint, to be comparable with the membrane thickness.

There could be no possible interplay between the structural degrees of freedom and the large-scale shape of the membrane without an energy term coupling these quantities. We consider the following, lowest-order interaction term:

$$f_{\rm int}^{(i)} = -\Lambda_i \left(u_i - a_i\right) \partial^2 h_i. \qquad (4)$$

It represents the coupling between the excess thickness and the spontaneous curvature. Like the spontaneous curvature term in $f_{\rm H}^{(i)}$, this term is allowed by symmetry *only* if the two monolayers forming the membrane are dissymmetric.

Finally, γ_0 is a line tension term that takes into account the microscopic interaction between the two domains (arising, e.g., from van der Waals forces).

For the sake of simplicity, we assume $B_1 = B_2 \equiv B$, $k_1 = k_2 \equiv k$ and $\Lambda_1 = \Lambda_2 \equiv \Lambda$, but we keep $\kappa_1 \neq \kappa_2$, $c_1 \neq c_2$, and $a_1 \neq a_2$. We shall discuss later on the orders of magnitude of the different terms. Note that the two-dimensional version of this model would be simply obtained by replacing dx by d^2x and ∂ by $\boldsymbol{\nabla}$.

2.1 Renormalized bending rigidity and spontaneous curvature

A straightforward effect of the coupling term $\Lambda(u_i - a_i)\partial^2 h_i$ is to renormalize, away from the joint, the bending rigidities and spontaneous curvatures [25]. Indeed, if we neglect ∂u_i (by assuming that the thickness is uniform far from the joint), the total free-energy density reduces to $\frac{1}{2}\kappa_i(\partial^2 h_i)^2 - \kappa_i c_i \partial^2 h_i + \frac{1}{2}B(u_i - a_i)^2 - \Lambda(u_i - a_i)\partial^2 h_i$. The latter yields, after minimization with respect to u_i, $u_i = a_i + (\Lambda/B)\partial^2 h_i$, and the energy density becomes $\frac{1}{2}\kappa_i'(\partial^2 h_i)^2 - \kappa_i' c_i' \partial^2 h_i$, with

$$\kappa_i' = \kappa_i - \frac{\Lambda^2}{B} \qquad (5)$$

$$c_i' = \frac{\kappa_i}{\kappa_i'}\, c_i \,. \qquad (6)$$

These are the effective bending rigidities and spontaneous curvatures of the membrane : the ones that would be measured in a macroscopic experiment and the ones that should appear in the Helfrich curvature energy.

2.2 Equilibrium equations

The Euler-Lagrange equilibrium equations associated with our elastic free-energy F are

$$\kappa_i\,\partial^4 h_i(x) = \Lambda\,\partial^2 u_i(x)\,, \tag{7}$$
$$k\,\partial^2 u_i(x) = B\,[u_i(x) - a_i] - \Lambda\,\partial^2 h_i(x)\,. \tag{8}$$

These equations should be solved with the correct number of boundary equations. First, there are three continuity equations at the joint:

$$\left(h_2 + \tfrac{1}{2}u_2\right)|_{x=0} = \left(h_1 + \tfrac{1}{2}u_1\right)|_{x=0} \tag{9}$$
$$\left(h_2 - \tfrac{1}{2}u_2\right)|_{x=0} = \left(h_1 - \tfrac{1}{2}u_1\right)|_{x=0} \tag{10}$$
$$\partial h_2|_{x=0} = \partial h_1|_{x=0}. \tag{11}$$

The first two conditions represent the requirement that the polar heads of the two membranes must match at the joint. They imply the continuity of both h_i and u_i. The third one, the slope continuity equation, must be imposed in order to avoid an infinite curvature energy, as explained in the introduction. Note that there is therefore no contact angle at the "microscopic" level in this model.

When calculating the variation δF associated with the variations $\delta u_i(x)$ and $\delta h_i(x)$, there are boundary terms in $x = 0$ in factor of $\delta u|_{x=0}$, $\delta h|_{x=0}$ and $\delta\partial h|_{x=0}$ (remember that u, h, and ∂h are continuous at the joint). These are boundary forces and torques. The associated equilibrium conditions are

$$f_1|_{x=0} + f_2|_{x=0} = 0\,, \tag{12}$$
$$f_1'|_{x=0} + f_2'|_{x=0} = 0\,, \tag{13}$$
$$\Omega_1|_{x=0} + \Omega_2|_{x=0} = 0\,, \tag{14}$$

corresponding to the vanishing of the total force relative to h, the total force relative to u, and the total torque relative to h, respectively, with

$$f_i = -\epsilon\left(\kappa_i\,\partial^3 h_i - \Lambda\,\partial u_i\right)\,, \tag{15}$$
$$f_i' = \epsilon\,k\,\partial u_i\,, \tag{16}$$
$$\Omega_i = \epsilon\left[\kappa_i\left(\partial^2 h_i - c_i\right) - \Lambda\,(u_i - a_i)\right]\,. \tag{17}$$

Here, $i \in \{1, 2\}$ indicates the domain where the quantity is calculated, and $\epsilon = 1$ if the quantity is calculated at the right-hand side boundary of its domain, while $\epsilon = -1$ if it is calculated at the left-hand side.

In addition, we assume that the domains $\mathcal{D}_i$ actually correspond to small regions in contact with larger membrane parts, in equilibrium under some unspecified boundary conditions and global constraints. These outer parts transmit boundary forces $f^{\rm ext}|_{x=\pm L}$, $f'^{\rm ext}|_{x=\pm L}$ and torques $\Omega_{\rm ext}|_{x=\pm L}$, which yield the equilibrium equations:

$$f_2|_{x=L} + f^{\rm ext}|_{x=L} = 0\,, \tag{18}$$
$$f_1|_{x=-L} + f^{\rm ext}|_{x=-L} = 0\,, \tag{19}$$
$$f_2'|_{x=L} + f'^{\rm ext}|_{x=L} = 0\,, \tag{20}$$
$$f_1'|_{x=-L} + f'^{\rm ext}|_{x=-L} = 0\,, \tag{21}$$
$$\Omega_2|_{x=L} + \Omega_{\rm ext}|_{x=L} = 0\,, \tag{22}$$
$$\Omega_1|_{x=-L} + \Omega^{\rm ext}|_{x=-L} = 0\,. \tag{23}$$

These conditions can be formally derived by adding to F the contribution :

$$\begin{aligned} F_{\rm ext} = {} & f^{\rm ext}|_{x=-L}\,h(-L) + f^{\rm ext}|_{x=L}\,h(L) \\ & + f'^{\rm ext}|_{x=-L}\,u(-L) + f'^{\rm ext}|_{x=L}\,u(L) \\ & + \Omega^{\rm ext}|_{x=-L}\,\partial h(-L) + \Omega_{\rm ext}|_{x=L}\,\partial h(L), \end{aligned} \tag{24}$$

and by equilibrating the boundary terms. Notice that Eqs. (9)–(23) correctly provide 12 boundary conditions for two integration domains subject to differential equations globally of the sixth order.

2.3 Equilibrium solutions

The general solutions of the set of linear differential bulk Eqs. (7)–(8) are:

$$\begin{aligned} h_i = {} & A_{i1} + A_{i2}\,x + \frac{1}{2}A_{i3}\,x^2 + \frac{1}{3}A_{i4}\,x^3 \\ & + A_{i5}\,\frac{\Lambda}{\kappa_i\,q_i^2}\,e^{q_i\,x} + A_{i6}\,\frac{\Lambda}{\kappa_i\,q_i^2}\,e^{-q_i\,x}, \end{aligned} \tag{25}$$
$$u_i = a_i + \frac{\Lambda}{B}\,A_{i3} + \frac{2\Lambda}{B}\,A_{i4}\,x + A_{i5}\,e^{q_i\,x} + A_{i6}\,e^{-q_i\,x}, \tag{26}$$

where $A_{i\alpha}$ are integration constants, and

$$q_i = \sqrt{\frac{\kappa_i'}{\kappa_i}}\,\sqrt{\frac{B}{k}}. \tag{27}$$

Since $q_i \approx \sqrt{B/k}$, we expect it to be of the order of the inverse of the membrane thickness (unless when $\kappa_i' \to 0$).

We see that the solutions are the sum of polynomials, which correspond to the solutions one would get in a pure Helfrich model plus relaxing exponentials, which correspond to the effect of the structural degrees of freedom. Since these exponentials appear also in h_i, they may affect the extrapolated angle at which the polynomials solutions meet the joint. This is the source of the effect we are interested in.

3 Detailed structure of the joint

To study the structure of the joint and its generic response to the constraints transmitted by the curvature elasticity of the membrane, it is enough to consider the situation in which two opposite far-away torques are applied: $\Omega^{\rm ext}|_{-L} = -\Omega^{\rm ext}|_{L} \equiv \Omega$. Remember that those torques are acting at the boundaries of the domains $\mathcal{D}_i$ and that they represent the effect of the pieces of membranes that

are outside the region we are studying. We set to zero the external boundary forces: $f^{\rm ext}|_{\pm L} = f'^{\rm ext}|_{\pm L} = 0$ (the latter would merely transmit extra torques). We also assume that the membrane domains are much larger than the "width" of the joint, i.e., $L \gg q_i^{-1}$.

3.1 Solution of the problem

With the above conditions, it follows from Eqs. (12)–(23) that $A_{i4} = 0$, $A_{16} = A_{25} = 0$ and that

$$A_{i3} = c'_i + \Omega/\kappa'_i \,. \tag{28}$$

Obviously, we may choose $A_{21} = A_{22} = 0$ by a simple translation and rotation of the reference frame. Requiring that the remaining boundary conditions be satisfied yields

$$A_{11} = \frac{\Lambda\,\mu}{\kappa_1\kappa_2}\,\frac{\kappa_2\,q_2^3 + \kappa_1\,q_1^3}{q_1^2\,q_2^2\,(q_1+q_2)}\,, \tag{29}$$

$$A_{12} = \frac{\Lambda\,\mu}{\kappa_1\kappa_2}\,\frac{B(\kappa_2-\kappa_1)}{k\,q_1\,q_2\,(q_1+q_2)}\,, \tag{30}$$

$$A_{15} = -\mu\,\frac{q_2}{q_1+q_2}\,, \tag{31}$$

$$A_{26} = \mu\,\frac{q_1}{q_1+q_2}\,, \tag{32}$$

with

$$\mu = a_1 - a_2 + \frac{\Lambda}{B}\left[c'_1 - c'_2 + \left(\frac{1}{\kappa'_1} - \frac{1}{\kappa'_2}\right)\Omega\right]. \tag{33}$$

We therefore find that the membrane shape h_i relaxes exponentially away from the joint with a characteristic length q_i^{-1} to a parabola of curvature A_{i3}, equal to the effective spontaneous curvature c'_i plus a deviation proportional to the applied external torque (Eq. (28)). The membrane thickness, u_i, relaxes exponentially to the value $a_i + (\Lambda/B)A_{i3}$, which is shifted with respect to a_i by an amount proportional to the curvature A_{i3}. These features can be seen in Fig. 1. Away from the joint, $h_i(x)$ tends to $H_i(x) = A_{i1} + A_{i2}\,x + \frac{1}{2}A_{i3}\,x^2$, as in the Helfrich model (for small membrane inclinations).

Although the joint essentially appears as a thickness matching, by extrapolating the large-scale solutions $H_i(x)$ up to $x = 0$, one finds a *non-zero contact-angle* (Fig. 1), $\theta \equiv \partial H_1|_{x=0} - \partial H_2|_{x=0}$, given by

$$\theta = A_{12} \neq 0\,. \tag{34}$$

As expected, θ is proportional to Λ: the coupling between the membrane shape and the structural degrees of freedom is necessary to obtain an effective contact-angle. Notice that there is also a mismatch in the extrapolated membrane height, $H_1|_{x=0} - H_2|_{x=0} \neq 0$, but we may neglect it because it is smaller than the membrane thickness.

3.2 Energy of the equilibrium configuration

By integrating F by parts and making use of the bulk equations, the total energy at equilibrium, $F \equiv F_0$, may be expressed as boundary terms only:

$$F_0 = \sum_{x=0^-,-L} \frac{1}{2}\left[f'_1\,(u_1-a_1) + f_1\,h_1 + (\Omega_1 - \kappa_1\,c_1)\,\partial h_1\right] + \sum_{x=0^+,L} \frac{1}{2}\left[f'_2\,(u_2-a_2) + f_2\,h_2 + (\Omega_2 - \kappa_2\,c_2)\,\partial h_2\right]. \tag{35}$$

Using the boundary conditions (9)–(23), and substituting the solution while taking the limit $Lq_i \gg 1$, the total energy may be cast into the following form:

$$F_0 = \sum_{i=1,2} L\left[\frac{1}{2}\kappa'_i\,A_{i3}^2 - \kappa'_i\,c'_i\,A_{i3}\right] + \gamma_0 + \gamma_1\theta + \frac{1}{2}\gamma_2\,\theta^2\,, \tag{36}$$

where

$$\gamma_1 = \frac{\kappa'_1\kappa'_2}{\kappa'_2-\kappa'_1}\left[\frac{B}{\Lambda}(a_1-a_2) + c'_1 - c'_2\right], \tag{37}$$

$$\gamma_2 = -\frac{B^{\frac{3}{2}}}{\sqrt{k}\,\Lambda^2}\left(\frac{\kappa'_1\kappa'_2}{\kappa'_2-\kappa'_1}\right)^2\left(\sqrt{\frac{\kappa_1}{\kappa'_1}} + \sqrt{\frac{\kappa_2}{\kappa'_2}}\right), \tag{38}$$

and γ_0 is the constant initially present in F. One recognizes in Eq. (36) the effective (large-scale) Helfrich energy calculated from the asymptotic curvatures A_{3i} (which are constant here) and the renormalized bending rigidities and spontaneous curvatures κ'_i and c'_i, plus an effective line energy $\gamma(\theta) = \gamma_1\theta + \frac{1}{2}\gamma_2\theta^2$.

Note that the large-scale curvatures A_{3i}'s and the effective contact-angle θ are controlled by the applied torque Ω (see Eqs. (28)-(33)). In fact, from Eqs. (30) and (33), one can show with a little algebra that

$$\Omega = -\gamma_2(\theta - \theta_0)\,, \tag{39}$$

where θ_0 is the extremum angle of $\gamma(\theta)$, given by

$$\theta_0 = \Lambda\sqrt{\frac{k}{B}}\,\frac{\kappa'_2-\kappa'_1}{\kappa'_1\kappa'_2}\left(\sqrt{\frac{\kappa_1}{\kappa'_1}} + \sqrt{\frac{\kappa_2}{\kappa'_2}}\right)^{-1}$$

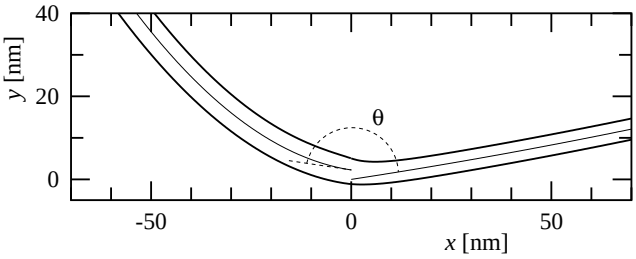

Fig. 1. Structure of the membrane in the vicinity of the joint. The upper and lower bold lines correspond to $h_i(x) + \frac{1}{2}u_i(x)$ and $h_i(x) - \frac{1}{2}u_i(x)$, respectively, where $i = 1$ for $x < 0$ and $i = 2$ for $x > 0$. The parameters are $\kappa_2 = 2\times10^{-19}$ J, $\kappa_1 = 5\,\kappa_2$, $c_1 = (50\,\text{nm})^{-1}$, $c_2 = 0.03\,c_1$, $B = 4\times10^{15}\,\text{J m}^{-4}$, $a_1 = 7$ nm, $a_2 = 5$ nm, $k = 10^{-1}\,\text{J m}^{-2}$, $\Lambda = 1.2\times10^{-2}\,\text{J m}^{-2}$, and $\Omega = 0$. The asymptotic large-scale solutions $H_i(x)$ are displayed as thin lines: their extrapolated contact-angle is $\theta = \theta_0 \simeq 17\,^\circ$. For a better view, the membrane has been rotated by $\theta/2$ counterclockwisely (and u_i has been corrected in order to yield the correct thickness when the slope is large).

$$\times \left[a_1 - a_2 + \frac{\Lambda}{B}\left(c_1' - c_2'\right)\right] = -\frac{\gamma_1}{\gamma_2}\,. \qquad (40)$$

Eq. (39) simply shows that the external torque Ω (which is transmitted up to the joint by the bending rigidity of the membrane) is equilibrated by the effective torque generated by the boundary line.

Note that we obtain $\gamma_2 < 0$. Because of this sign, the function $\gamma(\theta)$ possesses a *maximum* in $\theta = \theta_0$ and not a minimum. This is not a problem, actually, because $\gamma(\theta)$ is only an excess energy, which does not exist by itself in the absence of a surrounding membrane. Hence, there is no stability criterion for $\gamma(\theta)$ alone [26]. The only condition physically required is that the total energy be *minimum* for $\Omega = 0$, or, equivalently (since θ is an affine function of Ω) for $\theta = \theta_0$. This is indeed the case for $L > q_i^{-1}$, since the first term of Eq. (36), which is obviously minimum for $A_{3i} = c_i$, i.e., for $\Omega = 0$, i.e., for $\theta = \theta_0$, is proportional to L, while $\gamma(\theta)$ is not.

4 Effective large-scale Helfrich model with a boundary crease

We have therefore shown that our "microscopic" model taking into account the membrane thickness structural degree of freedom is equivalent, *at the coarse-grained level*, to the following (pure) Helfrich model supplemented by an anisotropic line energy for the effective joint contact-angle $\theta \equiv \partial h_1|_{x=0} - \partial h_2|_{x=0}$ (that must be considered as free to adjust to equilibrium):

$$F^{\text{eff}} = \sum_{i=1,2} \int_{\mathcal{D}_i} dx \left[\frac{\kappa_i'}{2}\left(\partial^2 h_i\right)^2 - \kappa_i'\, c_i'\, \partial^2 h_i \right] + \gamma_0' + \frac{1}{2}\gamma_2 \left(\theta - \theta_0\right)^2 , \qquad (41)$$

where $\gamma_0' = \gamma_0 - \frac{1}{2}\gamma_1^2/\gamma_2 > 0$. Here, $h_i(x)$ does not describe any longer the height profile of the membrane *midplane*, it simply describes the membrane as a whole, since at the level of Helfrich's description the whole bilayer is treated as a pure mathematical surface.

Let us detail the equivalence between the two models at the coarse-grained level. The equilibrium equations and boundary conditions at the joint, for the effective Helfrich model with energy F^{eff}, are

$$\partial^4 h_i(x) = 0\,, \qquad (42)$$

$$h_2|_{x=0} = h_1|_{x=0}\,, \qquad (43)$$

$$\partial h_2|_{x=0} = \partial h_1|_{x=0} + \theta\,, \qquad (44)$$

$$\bar{f}_1|_{x=0} + \bar{f}_2|_{x=0} = 0\,, \qquad (45)$$

$$\bar{\Omega}_1|_{x=0} = -\gamma'(\theta) = -\bar{\Omega}_2|_{x=0}\,, \qquad (46)$$

with, now, $\bar{f}_i = -\epsilon\,\kappa_i \partial^3 h_i$ and $\bar{\Omega}_i = \epsilon\,\kappa_i(\partial^2 h_i - c_i)$, ϵ being defined as previously. We see indeed that since ∂u_i tends to zero far from the joint, Eq. (7) is equivalent at the coarse-grained level to Eq. (42), and that the effective torque equilibrium equation (39) is equivalent to Eq. (46). The continuity Eq. (44) is postulated by the very definition of θ (which becomes a free parameter). Finally, Eqs. (43) and (45) are only approximately verified, but with a very good precision since we have seen that the height mismatch in the extrapolated large-scale solutions is smaller than the membrane thickness.

Note that Eq. (46) shows that θ_0 is the equilibrium (effective) contact-angle of the joint, attained when no torque is transmitted by the membrane, i.e., when the membrane is curved on both sides of the joints at its spontaneous curvature. This corresponds to the situation shown in Fig. 1.

In the limit $\Lambda \to 0$ (in which u_i becomes decoupled from the membrane shape h_i), we should recover the standard slope continuity condition. This is indeed the case, since Eqs. (38) and (40) yield then $\theta_0 \to 0$ and $\gamma_2 \to \infty$. We also obtain $\gamma_0' \to \gamma_0 + \frac{1}{4}\sqrt{Bk}\,(a_1 - a_2)^2$, which is simply the sum of the bare line tension and the elastic energy associated with the thickness mismatch in the absence of any coupling.

Finally, note that we have verified the equivalence of the large-scale behavior of models F and F^{eff} for arbitrary external forcings (including external forces in addition to external torques) by numerically solving the two boundary-value problem and comparing the solutions far from the joint.

5 Orders of magnitude

Let us discuss the orders of magnitude of the various parameters for a joint between two domains with a large thickness mismatch, e.g., as it is the case in the junction between biological membranes and rafts [19,20]. For biological membranes $\kappa_2 = 2 \times 10^{-19}\,\text{J}$ and $a_2 = 5\,\text{nm}$ are standard values [15]. Since rafts are known to be thicker and more ordered than normal membranes, we take $a_1 = 6\,\text{nm}$ and $\kappa_1 = 5\,\kappa_2$. From the area-stretching coefficient $k_s \simeq 0.1\,\text{J}\,\text{m}^{-2}$ [1] and the volume conservation relation $B \simeq k_s/a_2^2$, we obtain $B \simeq 4 \times 10^{15}\,\text{J}\,\text{m}^{-4}$. To estimate k, we assume that the relaxation length of u_i is comparable with the membrane thickness, which yields $k \simeq k_s$. These values are used in Fig. 1.

If the two monolayers are identical, we must set $c_i = 0$ and $\Lambda = 0$ by virtue of the resulting up-down symmetry, and hence there is no contact-angle effect within the present model. For asymmetric membranes, the values of the spontaneous curvature radii c_i^{-1} may range between several hundred of micrometers to a few tenth of nanometers, depending on the difference in lipid composition or inclusion concentrations between the two monolayers.

We must now estimate the parameter Λ. By comparing the terms $\kappa_i\, c_i \partial^2 h_i$ of f_{H} and $\Lambda(u_i - a_i)\partial^2 h_i$ of f_{int}, we see that Λ measures the dependence of the spontaneous curvature in the membrane thickness. We expect this dependence to be significant, since it is well-known that the spontaneous curvature of monolayers is (qualitatively) related with the effective conical shape of its constituents [1]. In the absence of any other information, let us assume that a 10 % change in the membrane thickness a (which is

Table 1. Values of the asymmetry-dependent constant Λ and the corresponding joint parameters as a function of the membrane spontaneous curvature radius c^{-1}.

c^{-1} [nm]	Λ [pN/nm]	$\lvert\theta_0\rvert$ [deg]	γ_0' [pN]	$R^\star$ [nm]
50	20	23	γ_0+5.002	96
300	3.3	2	γ_0+5.001	0.7
10^4	0.01	6×10^{-3}	γ_0+5	6×10^{-6}
0	0	0	γ_0+5	0

a large variation) may change the spontaneous curvature c by an amount comparable with the spontaneous curvature itself. This yields the estimate $\Lambda\times0.1\,a\simeq\kappa\,c$, which, with $\kappa\simeq5\times10^{-19}\,\mathrm{J}$ and $a\simeq5\,\mathrm{nm}$, gives $\Lambda\simeq10^{-9}\,\mathrm{J\,m^{-1}}\times c$. As shown in Table 1, it follows that significant contact-angles should only be expected for strong spontaneous curvatures. We see also that the contribution to the effective line tension depends very weakly on Λ.

5.1 Rigidity of the crease

To determine the angular rigidity of the joint, we can estimate the curvature radius $R^\star$ which must be applied to the joint in order to obtain an angular variation of 0.1 rad ($\simeq5.7\,\mathrm{deg}$). From Eq. (39), we obtain $R^\star\simeq\kappa/(\gamma_2\times.1)$ (see Table 1). We see that even for large values of Λ, $R^\star$ is quite microscopic; hence, the joint appears as extremely rigid. In consequence, we may almost view θ_0 as a *prescribed* contact-angle.

6 Discussion and conclusions

The present study shows that if the structural distortions arising within the joint between membrane domains are *coupled* with the membrane shape, then one should generically expect, in the large-scale elastic description, an effective slope discontinuity θ. The boundary line energy should then be considered, in general, a function $\gamma(\theta)$.

It should be noted, however, that if an extremely sharp extremum occurs in $\gamma(\theta)$ for $\theta_0=0$, then one effectively recovers the usual slope continuity condition and one should not bother about the angular dependence of $\gamma(\theta)$. The situation is therefore subtle and it is essential to consider the conditions for which either $\theta_0\neq0$ or the extremum of $\gamma(\theta)$ is shallow (compared to the torques produced by macroscopic elastic distortions).

It is not likely that the extremum of $\gamma(\theta)$ be effectively shallow. Indeed, finite apparent angular discontinuities must be resolved within the joint by strong continuous distortions, and the latter will always cost energies very large compared to those needed to curve the membrane on a macroscopic scale. It is thus more promising to look for $\theta_0\neq0$, but this is possible only for membranes with broken up-down symmetry, hence membranes bearing a spontaneous curvature. This is one of the reasons for the choice of the specific structural model studied here.

In fact, in this paper, we have examined the consequences of the most elementary boundary distortion: the membrane thickness matching (occurring, e.g., at a raft boundary). For the sake of simplicity, we have considered homogeneous membranes and we have assumed a *linear* coupling between the thickness and the shape of the membrane (the latter requiring the broken up-down symmetry). We have demonstrated, within this model, the existence of an effective anisotropic line tension $\gamma(\theta)$ and we have shown that it has such a sharp extremum θ_0 that the latter can be considered almost as a prescribed *contact-angle*. We have obtained $\theta_0\simeq0$ for membranes with macroscopic curvature radii, but θ_0 finite, for membranes with microscopic curvature radii. This is indeed interesting, because biological membranes, and especially rafts are known to be very asymmetric, with sphingomyelin and glycosphingolipids enriched in the exoplasmic leaflet and glycerolipids in the cytoplasmic leaflet [6]. Curvature radii of a few tenth of nanometers, as in Table 1, are thus plausible, and biological rafts could be expected to have contact-angles as large as 10—20°.

One should bear in mind that we have used a continuous model to investigate the effect of nanometric scale distortions. This is actually the limit of validity of continuous membrane models, and one should not expect better than semi-quantitative results. Besides, there are many other non-linear terms that might be taken into account, and also many other structural degrees of freedom. Real contact-angle might therefore be significantly stronger, or smaller, than what we have estimated here; experiments, or numerical simulations (e.g., with coarse-grained molecules) should be the best way to give a quantitative answer. Note also that we have neglected, for the sake of simplicity, the higher-order terms proportional to ∂^2u and $(\partial^2u)^2$ which have been investigated in [21]: they certainly would renormalize our results but cannot, for symmetry reasons, be the direct source of an effective contact-angle.

An interesting effect that we have neglected here is the possibility that the boundary will recruit dilute impurities and accumulate them in the joint, in order to relax some of the microscopic distortions. Since such impurities will in general have different concentrations in the two monolayers, they will locally enhance, within the joint, the local spontaneous curvatures and thus the local coupling constant Λ, yielding again finite contact-angles (even for up-down symmetric host membranes). These impurities could also soften the elasticity of the boundary distortions.

References

1. Israelachvili J. N., *Intermolecular and Surface Forces* (Academic Press, London, 1992).
2. Alberts B., Johnson A., Lewis J., Raff M., Roberts K. and Walter P. *Molecular Biology of the Cell* (Garland, New York, 2002).
3. Baumgart T., Hess S. T. and Webb W. W., Nature **425**, (2003) 821.
4. S. Leibler and D. Andelman, J. Phys. **48**, 2013 (1987).

5. M. Seul and D. Andelman, Science **267**, 476 (1995).
6. Simons K. and Ikonen E., Nature **387**, (1997) 569.
7. Anderson R. G. and Jacobson K., Science **296**, (2002) 1821.
8. Lipowsky R., J. Phys. II France **2**, (1992) 1825.
9. Jülicher F. and Lipowsky R., Phys. Rev. E **53**, (1996) 2670.
10. Allain J.-M. and Ben Amar M. Physica A **337**, (2004) 531.
11. Andelman D., Kawakatsu T. and Kawasaki K., Europhys. Lett. **19**, (1992) 57.
12. Jiang Y., Lookman T. and Saxena A., Phys. Rev. E **61**, (2000) 57.
13. Kumar P. B. S., Gompper G. and Lipowsky R., Phys. Rev. Lett. **86**, (2001) 3911.
14. Allain J.-M., Storm C., Roux A., Ben Amar M. and Joanny J.-F., Phys. Rev. Lett. **93**, (2004) 158104.
15. Mouritsen O. G., *Life—as a matter of fat* (The frontiers collection, Springer, Berlin, 2005).
16. Diamant et al., Phys. Rev. E **63**, (2001) 061602.
17. Helfrich W., Z. Naturforsch. C **28**, (1973) 693.
18. R. Goetz, G. Gompper and R. Lipowsky, Phys. Rev. Lett. **82**, 221 (1999).
19. Gandhavadi M., Allende D, Vidal A, Simon S. A. and McIntosh T. J., Biophys. J. **82**, (2002) 1469.
20. Lawrence J. C., Saslowsky D. E. , Edwardson J. M. and Henderson R. M., Biophys. J **84**, (2003) 1827.
21. Kuzmin P. I., Akimov S. A., Chizmadzhev Y. A., Zimmerber J. and Cohen F. S., Biophys. J. **88**, (2005) 1120.
22. Fournier J.-B., Eur. Phys. J. B **11**, (1999) 261.
23. Huang H. W., Biophys. J. **50**, (1986) 1061.
24. Dan N., Pincus P. Safran S. A., Langmuir **9**, (1993) 1061.
25. A similar effect was obtained in another context in: Leibler S., J. Physique **47**, (1986) 507.
26. This is reminiscent of the wetting surface energies in liquid crystals, which may also be separately unbounded: see, e.g., Sluckin T. J. and Poniewierski A., Phys. Rev. Lett. **55**, (1985) 2907; Seidin R., Hornreich R. M. and Allender D. W., Phys. Rev. E **55**, (1997) 4302.